**TITLE**

# A DIABETIC MICE MODEL FOR STUDYING SKIN WOUND HEALING

Carlos Poblete Jara[5], Guilherme Nogueira[3,4], Joseane Morari[3,4], Thaís Paulino do Prado[1,3,4], Renan de Medeiros Bezerra[1,3,4], Bruna Bombassaro[3,4], Lício A. Velloso[2,3,4], William Velander[5], Eliana Pereira de Araújo[1,3,4]

[1] Faculty of Nursing, [2] Faculty of Medical Sciences, [3] Laboratory of Cell Signaling, Obesity and Comorbidities Research Center, [4] University of Campinas, Brazil, [5] Department of Chemical and Biomolecular Engineering, University of Nebraska-Lincoln, Lincoln, NE, USA

Corresponding author:

Eliana P. Araújo,

Faculty of Nursing

University of Campinas, Brazil

E-mail: eraujo@unicamp.br

Short running title: **Mice model for skin wound healing**

*Keywords: animal model, high-fat-diet, streptozotocin, aging, wound healing*

**ABSTRACT**

Advances in wound treatment depend on the availability of animal models that reflect key aspects of human wound healing physiology. To this date, the accepted mouse models do not reflect defects in the healing process for chronic wounds that are associated with type two diabetic skin ulcers. The long term, systemic physiologic stress that occurs in middle aged or older type 2 diabetic patients is difficult to simulate in preclinical animal model. We have strived to incorporate the essential elements of this stress in a manageable mouse model: long term metabolic stress from obesity to include the effects of middle age and thereafter onset of diabetes. At six-weeks age, male C57BL/6 mice were separated into groups fed a Chow and High-Fat Diet for 0.5, 3, and 6 months. Treatment groups included long term, obesity stressed mice with induction of diabetes by streptozotocin at 5 months, and further physiologic evaluation at 8 months old. We show that this model results in a severe metabolic phenotype with insulin resistance and glucose intolerance associated with obesity and, more importantly, skin changes. The phenotype of this older age mouse model included a transcriptional signature of gene expression in skin that overlapped that observed with elderly patients who develop diabetic foot ulcers. This unique old age phenotype result contrasts with current non-obesity stressed mice models with induced diabetes at 4 months or younger which do not reflect the pathologic type 2 human phenotype.

## INTRODUCTION

Diabetes mellitus (DM) is a chronic metabolic disease characterized by hyperglycemia that results from deficiencies in insulin secretion and/or action. It is one of the major global health problems affecting over 463 million people worldwide and projecting an increase to 578 million by the end of 2023(1). As a chronic and refractory disease, DM affects every tissue and organ in the body, including the skin. Studies show that up to two-thirds of diabetic patients have skin problems at some point during their lifetime (2). There are several mechanisms behind DM-associated skin abnormalities, which include, but are not restricted to, oxidative stress, abnormal regulation of inflammatory products, impaired angiogenesis, and impaired growth factor production (3).

During the course of DM, two features seem central to explain the greater risk for development of skin disease: i, an accelerated skin aging (2, 4) and ii, an increased risk for development of secondary infections, which is particularly important in diabetic foot ulcers (DFU). DFU is the most common complication affecting DM patients; it increases the risk for development of osteomyelitis, which can lead to lower extremity amputations (5, 6) . Treating DFU has proven difficult as it results from a complex pathophysiology (6). Moreover, due to ethical concerns, trials for new therapeutic interventions in humans are limited, which delays the development of effective strategies to treat this condition. Therefore, testing new approaches to treat DFU must rely, at least during early phases, on the existence of appropriate experimental models.

Over the years, several experimental models have been employed in studies aimed at evaluating interventions for treating DFU. These include spontaneous autoimmune DM in rodents, genetically induced DM models; diet-induced DM models and pharmacologically induced DM models (7-9). Regardless of the benefits obtained with each of these models, they all have particular limitations. One important limitation that occurs in virtually all

models employed to date relies on the fact that they do not exhibit simultaneously two important features that are common to most patients with DFU; severe metabolic dysregulation and accelerated skin aging. Ideally, an experimental model for studying DFU should have close similarities to the clinical and pathological landscape of human DFU. In this study, we describe a model in which DM and aging result in skin alterations that display great similarities with those found in aging humans.

## RESULTS

### Diabetes induction

5-month old C57BL/6J mice were fed on HFD for 3 months when five low-dose injections of streptozotocin (STZ) (50 mg/kg, i.p.) were performed (Fig. 1a). Our results showed that after four weeks from STZ injections, HFD *diabetic* (HFD DM+) mice increased blood glucose levels up to 500mg/dL (489.7 mg/dL HFD DM+ vs 143 mg/dL age-matched non-diabetic mice, *p value* <0.0001). In addition, our result showed Chow diet did not affect fasting glycemia during the 8-month of analysis (Figure 1b, black bars). However, the 8-month old mice fed on HFD increased fasting glycemia compared to diet-paired 2.5-month old group (from 166 mg/dL in young to 206 mg/dL in older mice, *p value* 0.0268) (Figure 1b, blue bars). Moreover, the 8-month old HFD DM+ group increased even more fasting glycemia (3 fold more after 3 months streptozotocin injections) compared to diet-paired 2.5-month old counterparts (from 166 mg/dL younger to 490 mg/dL in older mice, *p value* <0.0001) (Figure 1b, red bars).

### Aging increases body mass and white adipose tissue deposition in mice.

Aging affects body mass (Figure 1c). Independently of food characteristics, mice fed on Chow or HFD increased Body mass during the 8 months of analysis (Figure 1c and Table 1, *p value* <0.0001). 8-month old mice fed on Chow diet increased body mass (from 22g to 33g, *p value* <0.0001) at rate 60-80mg/day (Supplementary 1b). Moreover, 8-month old mice fed on HFD increased body mass (from 25g to 49g, *p value* <0.0001) at rate 130-170mg/day (Supplementary 1b). However, after streptozotocin injections, HFD DM+ mice decreased body mass (from 36g to 30g, *p value* 0.0173) at a rate 70 mg/day (Supplementary 1b).

In addition, we found increased epididymal white adipose tissue (WAT) mass in older 5- and 8-month old mice fed with Chow diet compared to younger 2.5-month old mice fed on Chow (from 0.16g to 0.64g, *p value* <0.0001). This increase represents a 4-fold WAT mass in the 8-

month old group fed with Chow diet compared with their younger counterpart (Figure 1d, black bars). We found this WAT mass increase following the Body Mass increase pattern (Supplementary 1a). Additionally, mice fed on HFD increased even more WAT mass (Figure 1d, blue bars). We found increased WAT in older 8-month old animals fed with HFD compared with younger HFD 2.5-month and 5-month old groups (from 0.48g to 1.94g, *p value* 0.0001). In the same way that Chow fed animals, the increased WAT mass represents 4-fold the WAT mass of younger mice fed on HFD (Figure 1d). As well as the Chow group, we found this increase in WAT mass also follows the Body Mass increment pattern (Supplementary 1a).

However, the biggest differences were found in older 8-month old HFD DM+. HFD DM+ mice decreased WAT mass compared to younger 5-month old diabetic mice (from 1.7g to 0.7g, *p value* 0.0005) representing 2.3-fold less WAT mass (Figure 1d, red bars). Interestingly, over the course of 3 months with induced diabetes beginning at 5 months' age, this decrease in WAT mass also follows the Body Mass decline pattern of the HFD DM+ animals (Supplementary 1a).

**The hyperglycemic phenotype includes both insulin deficiency and polyphagia in HFD DM+.**

We explored how aging affects insulin levels and polyphagia. In 2.5-month old mice fed on chow diet showed 0.4 ng/mL insulin levels while 2.5-month old HFD mice showed 0.9 ng/mL insulin levels with no polyphagia. In 8-month old mice fed on chow diet showed 0.35 ng/mL insulin levels while 8-month old mice fed on HFD presented as 1.1 ng/mL insulin levels with no polyphagia. However, 8-month HFD-diabetic mice (HFD DM+) presented 0.3ng/mL insulin levels (Figure 1e) with polyphagia (Figure 1f).

8-month old HFD mice increased Food intake compared to 2.5-month old HFD mice (from 3g/day to 4g/day, *p value* 0.0232, Figure 1f). 8-month old HFD DM+ mice further increased

Food intake to 5g/day (*p value* <0.0001, Figure 1f). In contrast, 8-month old Chow diet mice showed no differences in Food intake (Figure 1f).

**Aging impacts Insulin and Glucose tolerance in mice fed on HFD diet.**

We investigated the contribution of aging to insulin sensitivity by Intraperitoneal injection of insulin (ITT) and glucose metabolism by Intraperitoneal injection of glucose (GTT) in Chow, HFD, HFD DM+ mice. Our results showed aging has a progressive and detrimental effect on insulin sensitivity and glucose metabolism in 8-month old HFD mice (Figure 1h-i). Increased glucose levels at 15, 30, 60, 90 and 120 min post insulin injection occurred compared to 2.5-month old HFD mice (*p value* <0.05, Figure 1h). GTT results in 8-month HFD mice also showed increased glucose levels 30 min after glucose challenge compared to 2.5-month HFD mice (*p value* <0.05, Figure 1i). Our results in 2.5, 5 and 8-month Chow fed mice showed no differences in the clearance pattern of plasma glucose except after 10 min post insulin injection (from 106 mg/dL to 150 mg/dL, *p value* 0.0260, Figure 1g left).

**Aging impacts gene expression associated with insulin pathway, obesity and aging.**

To better understand the effect of aging in the skin of Chow, HFD and HFD DM+ mice, we screened 3 different gene arrays: Aging, Insulin Pathway and Obesity.

Column A. Figure 1J shows the expression of age-associated genes in the skin of 8-month old animals relative to 2-month old counterparts. 8-month old Chow animals overexpressed *C3ar1* (8-fold), *Gsta1* (5-fold), and *Ccr1* (4-fold). In addition, 8-month old HFD animals specifically overexpressed *Calb1* (42-fold), *C5ar1* (30-fold), and *C3ar1* (26-fold). Skin from 8-month old HFD DM+ mice specifically overexpressed *Bub1b* (7-fold), *S100a8* (6-fold), and *Lmnb1* (5-fold).

Column B. Figure 1J shows the expression of Insulin-associated genes in the skin of 8-month old animals relative to 2-month old counterparts. 8-month old Chow animals

overexpressed *Lep* (9-fold), *Fos* (9-fold), and *G6pc* (8-fold), the HFD animals overexpressed *Lep* (50-fold), *G6pc2* (15-fold), and *Fos* (7-fold), and the HFD DM+ specifically overexpressed *Bub1b* (7-fold), *S100a8* (6-fold), and *Lmnb1* (5-fold).

Column C. Figure 1J shows the expression of Obesity-associated genes in the skin of 8-month old animals relative to 2-month old counterparts. 8-month old Chow animals specifically overexpressed *Thrb* (207-fold), *Ntsr1* (20-fold), and *Apoa4* (16-fold), the HFD animals overexpressed *Oprm1* (182-fold), *Lep* (48-fold), and *Adipoq* (25-fold), and the HFD DM+ overexpressed *Adipoq* (28-fold), *Ucp1* (15-fold), and *Lep* (13-fold).

**Aging affects pancreatic Insulin 1 and 2 expressions in mice fed on HFD.**

*Ins1* and *Ins2* genes encode for insulin 1 and 2, peptides that are vital in the regulation of carbohydrate and lipid metabolism. Our result showed that total *Ins1&2* gene expression increased in **pancreatic** tissue in 5-month old mice fed on HFD (Figure 1k). After streptozotocin injections, the HFD DM+ mice decreased pancreatic total *Ins1&2* gene expression (Figure 1k).

**Aging affects the accumulation of intrahepatic and dermal fat in HFD and Chow fed mice.**

Both the accumulation of intrahepatic fat (Hepatic steatosis) and insulin resistance are associated with liver metabolic dysfunction (10, 11). For this reason, we explored intrahepatic fat percentage in HFD DM+. Figure 1m shows the histological presence of intrahepatic fat. After 8 months on Chow diet, intrahepatic fat increased from 7% to 11% when comparing to 2-month old mice (*p value* <0.0001). 8-month old HFD mice had increased intrahepatic fat percentage from 19% to 38% (*p value* <0.0001). HFD DM+ animals increased from 19% to 25% (*p value* 0.0148).

Dermal white adipose tissue (dWAT), occurs in the dermis underlying the reticular dermis (12), and participates in thermogenesis, wound healing and immune defense against infection (13). We investigated dermal fat deposition in mice fed on Chow, HFD and HFD DM+. Figure 1n shows the histological presence of dWAT. 8 months Chow and HFD animals increased dWAT relative to both 2- and 5-month old mice (*p value* <0.0001). In contrast, HFD DM+ mice decreased dWAT relative to 5-month old HFD mice (*p value* <0.0001).

**HFD and hyperglycemia affects body mass in HFD DM+ mice.**

In our previous studies of mice less than 5-month age, we have shown that HFD affects body mass (14-17) (). Figure 2a shows that after only 2 weeks on HFD, mice had 13% increased body mass as compared to the Chow diet group (24.6g HFD vs 21.9g Chow, *p value* <0.0001 ). 3 months additional feeding on HFD resulted an increase of 35% of body mass compared to Chow diet (37.8g HFD vs 27.9g Chow, *p value* 0.0024). A total of 6 months HFD increased body mass by 47% compared to Chow diet mice (49.1g vs 33.5g, *p value* <0.0001). In contrast, HFD DM+ after a total of 6 months on HFD had decreased 39% body mass compared with their non-diabetic HFD counterparts (30.1g HFD DM+ vs 49.1g HFD, *p value* <0.0001).

**HFD DM+ have both decreased insulin expression and circulating insulin.**

Our result showed that after post Streptozotocin treatment, HFD DM+ decreased Pancreatic *Ins1* and *Ins2* expression (0.05-fold change, *p value* 0.0335) at 8 months of age (Figure 2b). Figure 2c shows fasting blood insulin levels. Mice fed for only 0.5 months on HFD beginning at 2 months age had increased fasting blood insulin levels compared to Chow animals (0.41ng/mL vs 1.3ng/mL, *p value* 0.0374). Mice after a total of 6 months on HFD increased insulin levels to 1.1ng/mL while Chow animals had 0.3 ng/mL (*p value* 0.0017). 8-month HFD DM+ (6 months on HFD) showed 0.3ng/mL.

We found mice fed on HFD for 3 months increased 37% Fasting blood glucose compared to Chow diet mice (190mg/dL vs 139mg/dL, *p value* 0.0021) (Figure 2d). After 6 months on HFD, mice had a 41% increased glucose levels compared to Chow mice (201mg/dL vs 142mg/dL, *p value* <0.0001). In contrast, HFD DM+ had 144% and 243% increased Fasting blood glucose when compared with age and HFD- and Chow, respectively (490mg/dL vs 201mg/dL vs 142mg/dL, *p value* <0.0001).

**Diabetic mice showed polyphagic food intake and polydipsic water intake.**

Our results showed HFD DM+ mice increased daily Food intake (Figure 2e). HFD DM+ mice displayed a 25% increased daily Food intake compared with their non-diabetic HFD counterparts (5g vs 4g, *p value* 0.0021). We found no differences in water intake (9mL vs 6mL, *p value* 0.0718) between Chow diet and HFD mice (Figure 2f). However, HFD DM+ showed polydipsic water intake compared either to Chow diet or their non-diabetic HFD counterparts (16g vs 9g, *p value* <0.0001) (Figure 2f). This difference in diabetic mice represents a 44% more daily water intake compared to the HFD mice and 63% more water intake compared to mice fed on Chow diet.

**HFD DM+ have decreased epididymal White Adipose.**

HFD mice increased WAT mass compared to Chow diet (480mg vs 156mg, *p value* 0.0002) (Figure 2g). This difference represents a 207% more WAT mass in HFD animals compared to the Chow group. An additional 3 months on HFD resulted a further 431% increase of WAT (1674mg vs 315mg, *p value* 0.0007) compared to Chow diet (Figure 2g). After 6 months on HFD, mice further increased WAT mass by 205% (1942mg vs 638mg, *p value* <0.0001) compared to Chow diet (Figure 2g). In contrast, 8-month HFD DM+ mice decreased WAT mass by 161% compared to their non-diabetic HFD counterparts (743mg vs

1942mg, *p value* <0.0001) (Figure 2g). We identified similar results of White adipose tissue mass after Body Mass correction (Figure 2h).

**HFD and HFD DM+ mice present chronic glucose intolerance.**

GTT results showed increased plasma glucose levels at 90 min (138mg/dL vs 189mg/dL) and 120 minutes (140mg/d vs 187mg/dL) after 0.5 months of HFD compared with Chow diet mice (*p value* <0.05) (Figure 2j). After 3 months of HFD feeding, mice increased plasma glucose levels at each time point of GTT sampling (0, 15, 30, 60, 90 and 120 min) (*p value* <0.05). 8-month old HFD mice (HFD for 6 months) also had increased plasma glucose levels at all time of GTT sampling (*p value* <0.0001). HFD DM+ mice presented higher plasma glucose levels (498mg/dL vs 364mg/dL) at all GTT time points compared to their age-matched HFD group (*p value* <0.0001). There were no differences in the AUC (from plasma glucose levels) of animals fed on HFD for 0.5 months (Figure 2k). After 3 months on HFD, the AUC increased 99% compared to Chow animals (*p value* 0.0010) (Figure 2k). HFD DM+ mice also showed a 170% AUC increase relative to the Chow diet group (*p value* <0.0001)(Figure 2k).

**HFD and HFD DM+ mice present chronic Insulin resistance.**

To determine the whole-body sensitivity to insulin, we measured blood glucose levels after intraperitoneal insulin administration (Figure l-m). ITT results showed that after 0.5 months of HFD plasma glucose levels increased at 5 min (175mg/dL vs 142mg/dL) and 15 min (108mg/dL vs 91mg/dL) compared to mice fed on Chow diet (*p value* <0.05) (Figure l). After 3 months on HFD the plasma glucose levels increased at 0 min (180mg/dL vs 153mg/dL), 5 min (214mg/dL vs 164mg/dL), and also 10 min (177mg/dL vs 122mg/dL) (*p value* <0.05).

After 6 months on HFD the plasma glucose levels were increased at all time points (*p value* 0.0001). 8-month old HFD DM+ mice (6 months on HFD) also presented higher plasma glucose levels at all time points (*p value* <0.0001). A constant rate of glucose disappearance was observed (kITT) (Figure 2m) where higher values indicate greater tissue insulin resistance (18, 19). As results, no kITT differences were observed after 0.5 months of HFD feeding (*p value* 0.0783) (Figure 2m) but kITT increased after 3 months on HFD (*p value* 0.0071) (Figure 2m). This kITT difference represents a 41% more in insulin resistance in HFD animals compared to the Chow group. HFD DM+ showed increased kITT values compared to age-matched Chow diet groups (*p value* 0.0274), but not when compared to the HFD group (Figure 2m). This kITT difference in HFD DM+ mice represents a 133% increase in insulin resistance compared to Chow diet mice but no difference with the HFD group (p valor 0.7867) (Figure 2m).

**Diet and glycemia impact gene expression associated with insulin pathway, obesity and aging.**

**Column A.** Figure 2i shows the expression of insulin-associated genes in the skin of 8-month old HFD animals relative to 8-month old Chow counterparts. After 2 weeks on HFD, skin tissue increased *Igfbp1* (3.2-fold), *G6pc* (2.5-fold), and *Ins1* (2-fold) more transcripts than their age-matched Chow diet counterparts. After 6 months on HFD, skin tissue overexpressed *G6pc2* (8.7-fold), *Lep* (8.5-fold), and *Ins1* (6 fold) more transcripts as well as downregulation of Akt1 (0.01 fold) when compared to their age-matched Chow diet counterparts (Figure 2i).

**Column B.** Figure 2i shows the expression of obesity-associated genes in the skin of 8-month old HFD animals relative to 8-month old Chow counterparts. After 2 weeks on HFD, skin tissue increased *Thrb* (26-fold), Apoa4 (8.5-fold), and *Sst* (4-fold). After 6 months

on HFD, skin tissue overexpressed *Oprk1* (17-fold), Drd2 (11-fold), and *Mc3r* (11-fold) (Figure 2i).

**Column C.** Figure 2i shows the expression of aging-associated genes in the skin of 8-month old HFD animals relative to 8-month old Chow counterparts**.** After 2 weeks on HFD, only 3 of 89 genes were >2-fold expressed: *Fcgbp* (3-fold), *Gsta1* (2.8-fold), and *Fcgr1* (2.3-fold) had increased expression. After 6 months on HFD, skin tissue from HFD mice increased expression of *Fcgr1* (16-fold), *C5ar1* (11-fold), and *C3ar1* (9-fold) (Figure 2i).

To confirm the above array results from skin samples, we assessed individual gene expression by PCR. Our PCR results showed increased for HFD (after 6 months feeding) of the expression of *Lep* (5.6-fold) as compared to Chow diet mice (*p value* 0.0011) and also 5.9 fold more *Lep* expression compared to HFD DM+ (*p value* 0.0011). After 6 months on HFD, an increase of 11.2-fold of *Ins1* as compared to Chow diet mice (*p value* 0.0003), and 10-fold as compared to HFD DM+ (*p value* 0.0001). *Akt1* was downregulated in both HFD and HFD DM+ mice (*p value* 0.0291). The inflammatory gene markers after, mice increased *Tnf*□ (*p value* 0.0008), *Il1β* (*p value* 0.0004) and *Il6* (*p value* 0.0156) after 6 months on HFD (Figure 2n).

**HFD and hyperglycemia affect intrahepatic fat deposition in mice.**

Our results showed that HFD and hyperglycemia both are associated with accumulation of intrahepatic fat percentage in mice (Figure 3a,c). Mice fed for 0.5 months on HFD had increased intrahepatic fat compared to age-matched Chow fed mice (19% vs 11% , *p value* <0.0001). Mice fed for 3 months on HFD also had increased intrahepatic fat compared to age-matched Chow fed mice (21% vs 13%, *p value* <0.0001). After 6 months on HFD, mice further increased intrahepatic fat compared to age-matched Chow fed mice (38% vs 9.3%, *p*

*value* <0.0001). In contrast, HFD DM+ had decreased intrahepatic fat percentage as compared to age-matched HFD fed mice (38% vs 25% , <0.0001) (Figure 3a,c).

**HFD and hyperglycemia affect dermal fat deposition in mice.**

Our histological analysis showed that HFD and HFD DM+ had different levels of accumulated dWAT (Figure 3b,d). Both mice with 0.5 months and 3 months on HFD had increased dWAT as compared to the Chow fed mice (*p value* <0.05). In contrast, HFD DM+ mice had decreased dWAT as compared to HFD group (*p value* <0.0001)(Figure 3b,d).

**A comparison of gene expression of diabetic human and HFD DM+ mice in skin.**

A Mouse Insulin Pathway array (Qiagen, PAMM-030Z) was used to compare 20-gene expression of skin samples with diabetic human and HFD DM+. Relative to non-diabetic skin samples, our analysis identified 10-common genes: *RRAS, SLC27A4, CFD, EIF4EBP1, GRB2, SORBS1, PTPN1, GSK3B, HRAS* and *BRAF* (Figure 4a).

We compared this 8-month old HFD DM+ model data to previously published data of 4-month old STZ-induced diabetic non-HFD mice. We identified 4 common genes increased between older and younger STZ-induced diabetic mice: *Pparg, Dok3,* Vega and *Grb2* (Figure 4a).

## DISCUSSION

Here, we described the metabolic phenotype of an experimental model that can be used to study skin wound healing in aging and DM. We showed that an experimental model that associates diet-induced obesity, aging and pharmacological induction of diabetes mellitus results in a severe metabolic phenotype with insulin resistance, reduced b-cell insulin expression and glucose intolerance and this is associated with changes in the skin that match the skin of aging humans with DM.

DM is a chronic metabolic disease that is associated with accelerated aging resulting in the damage of several tissues and organs in the body including steatosis of the liver (20-22). The skin is an important target of the metabolic, vascular, immunological, and neural abnormalities that result from a poorly controlled DM. The processes for the development of these problems are not yet entirely elucidated (4, 23). Diminished lamellar body synthesis, lipid production of epidermal cells, and decreased hydration have also been correlated with persistent hyperglycemia, take the lead to the deterioration of the cutaneous barrier function, and turning the skin prone to dryness and infections (24, 25) .Furthermore, increased oxidative stress and low-grade inflammation are associated with the development of skin lesions from diabetes (10.2174/157339911797415585). Thus, in our animal model, we observed changes in the transcripts of important aging intermediaries that could result in alterations in the skin (Figure 4a). Moreover, we observed decreased in transcripts involved in insulin action and obesity. Pro-inflammatory cytokines are crucial in regulating the inflammatory process during cutaneous wound healing, that can prolong the inflammatory phase and inhibit healing progression (6, 26, 27). Furthermore, some transcripts associate with diet-induced obesity, aging and pharmacological induction of diabetes, as a Gsk3b, was observed in this work (Figure 5). Gsk3b performs as a negative controller in Wnt signaling (28). Wound healing stimulate Wnt signaling and this canonical signaling contributes to each

sequential period of the healing process from the management of the inflammatory phase and programmed cell death to the mobilization of stem cell pools within the wound (29). Likewise, c-Jun and Serpina-1 were shown to be modulated in the skin of this animal model (figure 5). C-Jun and Serpina-1 are intimately involved in the inflammatory as well as the proliferative phase of the wound healing process (30).

DFU is the most common skin condition associated with diabetes and, because of the lack of optimal therapeutic interventions, it leads to prolonged periods of inactivity, high risk of infections and eventually the need for amputations (31-33). The development of new therapeutic interventions that could promote faster and more effective wound healing could improve life quality of affected patients, reducing the risk for severe outcomes. However, testing new agents that could improve the therapeutics of DFU is frequently a problem as ethical issues impose a number of restrictions. Thus, at least in early phases of testing, animal models can provide a fast and effective approach to identify candidates with high chance of success.

Most animal models used to date do not match clinical conditions frequently seen in humans with DM and DFU. Usually mice models with severe diabetes, develop such condition early in life, thus, the important component of aging is missing (7-9). Conversely, in models of DM induced by the consumption of energy dense diets lead to a chronic condition that can be sustained until late life; however, under these circumstances, metabolic abnormalities are generally mild (34-36).

## CONCLUSION

Here we present an old age, obesity stressed mouse model with old age onset of diabetes. We showed that mice submitted to a 8 month long physiologic stress developed severe metabolic abnormalities associated with aging, long-term obesity and subsequent onset of diabetes. For example, tissue abnormalities such as hepatic steatosis occurred but the most striking was a skin phenotype which histologically and transcriptionally could be compared to aging DM patients. Thus, this unique model is perhaps useful to therapeutic development for the treatment of human decubitus ulcers.

## METHODS

### RT2 Profiler PCR arrays

Gene expression was analyzed as previously described (37) . Briefly, Gene expression was obtained using 3 different 96-well RT2 Profiler PCR Arrays, Mouse Wound Healing (REF. No PAMM-121Z), Mouse Insulin Pathway and Obesity array from Qiagen, according to the manufacturer's instructions. For each treatment group and time point, the array was run three times. RT-PCR was run on a StepOnePlus™ Real-Time PCR system (Thermo Fisher Scientific). For data normalization, Hsp90ab1 was selected as the reference gene based on data from the Mouse Housekeeping Genes RT² Profiler™ PCR Array (REF. No. 330231 PAMM-000ZA, Qiagen, Maryland, USA) and subsequent calculation of M values using the geNorm software (Biogazelle NV, Gent, Belgium). StepOne Software v.2.3 was used for data analyses, and gene expression was calculated with the ΔΔCt method. A gene was assumed to be differentially expressed if there was at least a twofold difference expression,

### Experimental model

Six-week-old male C57BL/6 mice were obtained from the Animal Facility of the University of Campinas. All mice were kept in individual cages at 21 ± 5 °C, in 12/12 h light/dark cycle, with water and chow or HFD (Table 2) *ad libitum*. In all experiments, control and intervention group mice were treated in the same experimental settings. All experiments were conducted according to the "Guide for the Care and Use of Laboratory Animals of the Institute of Laboratory Animal Resources, US National Academy of Sciences" and were approved by the Ethics Committee (CEUA IB/UNICAMP n° 5425-1/2019).

**Dietary interventions**

Eight-week-old mice were separated into seven groups. Three groups fed with Chow diet (base-line control). The remaining four groups were fed with High-Fat diet (HFD) for 2, 12 or 24 weeks (diets composition in Table 1, experimental design in Figure 1). Mice were analyzed for Intraperitoneal Insulin Tolerance test (ITT) and Intraperitoneal Glucose Tolerance Test (GTT). Then, mice were subjected to lethal anesthesia and tissues specimens were extracted for analyses.

**Metabolic characterizations**

For ITT, mice were fasted as previously described (Bombassaro et al., 2019). Tail blood was collected for basal glucose evaluation. A solution of insulin (1.5 U/kg body weight) was administrated via intraperitoneal and blood was collected from tail vein after 5, 10, 15 and 20 minutes. For GTT, mice were submitted to fasting protocol according previously described (38). Basal glucose concentration was determined from collected tail blood. A solution of 20% glucose (2.0 g/kg body weight) was administrated via intraperitoneal and blood from tail vein was collected after 15, 30, 60, 90 and 120 minutes. In both tests, blood glucose concentration was measured using handheld glucometer.

**Diabetes Mellitus induction protocol**

At 22 weeks of age, one group on HFD was induced to diabetes mellitus (DM) with Streptozotocin (STZ). Mice were fasted for 4h before daily intraperitoneal injections of STZ (50 mg/kg). STZ was daily and freshly dissolved in 0.1 M sodium citrate buffer, pH 4.5, and the dose volumes for each mouse were calculated by Labinsane app (Jara et al., 2021) STZ injections were made for five consecutive days (low multiple-dose protocol). One group on HDF and one on chow were injected sodium citrate buffer and served as control.

Induced DM state was assessed after four weeks using an OptiumTM mini (Abbott Diabetes Care, Alameda, CA, USA) handheld glucometer with appropriate test strips. Blood glucose levels were measured by blood from tail vein. Mice whose blood glucose levels exceeded 300 mg/dL after treatment were considered *diabetic*.

**Diary food intake and mice weight measurements (Renan)**

One week before ITT and GTT experiments of each group, the mice were submitted to food and weight measurements to avoid more distress from the procedures that could interfere in their intake. The mice were fasted for 12 hours overnight and then weighed for five consecutive days at the same hour, their food was also weighed at the same time to analyze calories intake and cumulative weight gain. In addition, the 24-week group with mice that were induced to a DM state also had their water intake measured in the same period.

**Tissue extraction**

Mice were submitted to fasting protocol according to previously described (Nogueira et al, 2020). Subsequently, mice were anesthetized with lethal doses of xylocaine and ketamine calculated by Labinsane App. Pancreas and fragments of dorsal skin (8.0 mm punch), liver, epididymal white adipose tissue, were extracted and prepared for molecular analysis or histological staining. Plasma samples was obtained from whole blood samples collected in EDTA pre-coated tubes, followed by centrifugation (3500 RPM, 15 minutes, room temperature), and were stored at −80 °C.

**Determination of glucose, and insulin**

Serum glucose was determined by the glucose oxidase method, as previously described (17). Serum insulin was determined by RIA, as described (18). Serum leptin was determined using an ELISA kit from Linco/Millipore (Billerica, MA) according to the recommendations of the manufacturer (39).

**Intraperitoneal glucose tolerance test**

After 6 h fasting, mice were anesthetized by an ip injection of sodium amobarbital (15 mg/kg body weight), and the experiments were initiated after the loss of corneal and pedal reflexes. After collection of an unchallenged sample (time 0), a solution of 20% glucose (2.0 g/kg body weight) was administered into the peritoneal cavity. Blood samples were collected from the tail at 30, 60, 90, and 120 min for determination of glucose and insulin concentrations (39).

**Insulin tolerance test**

Insulin (1.5 U/kg) was administered by ip injection, and blood samples were collected at 0, 5, 10, 15, 20, 25, and 30 min for serum glucose determination. The rate constant for glucose disappearance during an insulin tolerance test (kITT) was calculated using the formula 0.693/t1/2. The glucose t1/2 was calculated from the slope of the least-square analysis of the plasma glucose concentrations during the linear decay phase (39).

For the histological analyses, fragments of liver, pancreas and skin tissues were processed and stained with hematoxylin and eosin as previously described.

## CONFLICTS OF INTEREST

No conflicts of interest

## AUTHOR CONTRIBUTIONS

CPJ: Conceptualization, Formal analysis, Methodology, Investigation, Writing - Original Draft, Writing - Review & Editing

GN: Conceptualization, Formal analysis, Methodology, Investigation

JM: Conceptualization, Formal analysis, Methodology, Investigation

TPP: Methodology and Investigation

RMB: Methodology and Investigation

LAV: Formal analysis, Writing - Review & Editing, Supervision

WV: Formal analysis, Writing - Review & Editing, Supervision

EPA: Conceptualization, Methodology, Formal analysis, Resources, Writing - Original Draft, Writing - Review & Editing, Supervision

**FIGURES**

**Figure 1a**

Schematic representation of experimental design. C57BL/6 mice were fed either with Chow Diet or High Fat diet. Some 5-month old HFD animals were treated with streptozotocin for Diabetes induction (HFD DM+ group) generating 2 HFD groups: a) HFD DM+ (T2DM-like) and b) HFD non-diabetic.

**Table 1**

| | | **Age (months)** | | | |
|---|---|---|---|---|---|
| **Body mass** | | 2.5 | 5 | 8 | *p value* |
| **Chow** | Mean (g) | 21.9 | 27.9 | 33.4 | <0.0001 |
| | SD | 1.3 | 1.8 | 1.7 | |
| **HFD** | Mean (g) | 24.8 | 37.8 | 49.1 | <0.0001 |
| | SD | 0.9 | 5.7 | 3.1 | |
| **HFD DM+** | Mean (g) | 24.4 | 36.0 | 30.1 | <0.0001 |
| | SD | 0.5 | 4.9 | 2.7 | |
| | *p value* | <0.0001 | 0.0024 | <0.0001 | |

**Table 2.** Macronutrient component of the diets.

| **Components** | **Chow (g)** | **High-fat diet (g)** |
|---|---|---|
| Starch | 427.5 | 199.5 |
| Protein (casein 85%) | 200 | 200 |
| Dextrinized corn starch | 132 | 132 |
| Sucrose | 100 | 100 |
| Soyabean oil | 40 | 40 |
| Lard | 0 | 228 |
| Fiber (celulose) | 50 | 50 |

| | | |
|---|---|---|
| Mineral mix (ain-93) | 35 | 35 |
| Vitamin mix (ain-93) | 10 | 10 |
| L-cystine | 3 | 3 |
| Choline bitartarate | 2.5 | 2.5 |
| **TOTAL** | **1000** | **1000** |

## REFERENCES


1. Saeedi P, Petersohn I, Salpea P, Malanda B, Karuranga S, Unwin N, et al. Global and regional diabetes prevalence estimates for 2019 and projections for 2030 and 2045: Results from the International Diabetes Federation Diabetes Atlas, 9(th) edition. Diabetes Res Clin Pract. 2019;157:107843.
2. Duff M, Demidova O, Blackburn S, Shubrook J. Cutaneous Manifestations of Diabetes Mellitus. Clinical Diabetes. 2015;33(1):40-8.
3. Burton JL. Dietary fatty acids and inflammatory skin disease. Lancet. 1989;1(8628):27-31.
4. Lima AL, Illing T, Schliemann S, Elsner P. Cutaneous Manifestations of Diabetes Mellitus: A Review. Am J Clin Dermatol. 2017;18(4):541-53.
5. Margolis DJ, Allen-Taylor L, Hoffstad O, Berlin JA. Diabetic Neuropathic Foot Ulcers: The association of wound size, wound duration, and wound grade on healing. Diabetes Care. 2002;25(10):1835-9.
6. Bermudez DM, Herdrich BJ, Xu J, Lind R, Beason DP, Mitchell ME, et al. Impaired biomechanical properties of diabetic skin implications in pathogenesis of diabetic wound complications. Am J Pathol. 2011;178(5):2215-23.
7. Rees DA, Alcolado JC. Animal models of diabetes mellitus. Diabetic Medicine. 2005;22(4):359-70.
8. King AJ. The use of animal models in diabetes research. Br J Pharmacol. 2012;166(3):877-94.
9. King A, Bowe J. Animal models for diabetes: Understanding the pathogenesis and finding new treatments. Biochem Pharmacol. 2016;99:1-10.
10. Nassir F, Rector RS, Hammoud GM, Ibdah JA. Pathogenesis and Prevention of Hepatic Steatosis. Gastroenterol Hepatol (N Y). 2015;11(3):167-75.
11. El-Zayadi AR. Hepatic steatosis: a benign disease or a silent killer. World J Gastroenterol. 2008;14(26):4120-6.
12. Driskell RR, Jahoda CA, Chuong CM, Watt FM, Horsley V. Defining dermal adipose tissue. Exp Dermatol. 2014;23(9):629-31.
13. Chen SX, Zhang LJ, Gallo RL. Dermal White Adipose Tissue: A Newly Recognized Layer of Skin Innate Defense. J Invest Dermatol. 2019;139(5):1002-9.
14. Carraro RS, Souza GF, Solon C, Razolli DS, Chausse B, Barbizan R, et al. Hypothalamic mitochondrial abnormalities occur downstream of inflammation in diet-induced obesity. Mol Cell Endocrinol. 2018;460:238-45.
15. Carraro RS, Nogueira GA, Sidarta-Oliveira D, Gaspar RS, Dragano NR, Morari J, et al. Arcuate Nucleus Overexpression of NHLH2 Reduces Body Mass and Attenuates Obesity-Associated Anxiety/Depression-like Behavior. J Neurosci. 2021;41(48):10004-22.
16. Bombassaro B, Ramalho AFS, Fioravante M, Solon C, Nogueira G, Nogueira PAS, et al. CD1 is involved in diet-induced hypothalamic inflammation in obesity. Brain Behav Immun. 2019;78:78-90.

17. Mendes NF, Gaspar JM, Lima-Júnior JC, Donato J, Jr., Velloso LA, Araújo EP. TGF-β1 down-regulation in the mediobasal hypothalamus attenuates hypothalamic inflammation and protects against diet-induced obesity. Metabolism. 2018;85:171-82.
18. Dragano NR, Marques A, Cintra DE, Solon C, Morari J, Leite-Legatti AV, et al. Freeze-dried jaboticaba peel powder improves insulin sensitivity in high-fat-fed mice. Br J Nutr. 2013;110(3):447-55.
19. Lee MY, Koh JH, Nam SM, Jung PM, Sung JK, Kim SY, et al. Short insulin tolerance test can determine the effects of thiazolidinediones treatment in type 2 diabetes. Yonsei medical journal. 2008;49(6):901-8.
20. Franceschi C, Garagnani P, Parini P, Giuliani C, Santoro A. Inflammaging: a new immune–metabolic viewpoint for age-related diseases. Nature Reviews Endocrinology. 2018;14(10):576-90.
21. Yang Z, Ming XF. mTOR signalling: the molecular interface connecting metabolic stress, aging and cardiovascular diseases. Obesity Reviews. 2012;13(S2):58-68.
22. Wang CY, Kim HH, Hiroi Y, Sawada N, Salomone S, Benjamin LE, et al. Obesity increases vascular senescence and susceptibility to ischemic injury through chronic activation of Akt and mTOR. Sci Signal. 2009;2(62):ra11.
23. Makrantonaki E, Jiang D, Hossini AM, Nikolakis G, Wlaschek M, Scharffetter-Kochanek K, et al. Diabetes mellitus and the skin. Reviews in Endocrine and Metabolic Disorders. 2016;17(3):269-82.
24. Sakai S, Kikuchi K, Satoh J, Tagami H, Inoue S. Functional properties of the stratum corneum in patients with diabetes mellitus: similarities to senile xerosis. British Journal of Dermatology. 2005;153(2):319-23.
25. Girach A, Manner D, Porta M. Diabetic microvascular complications: can patients at risk be identified? A review. International Journal of Clinical Practice. 2006;60(11):1471-83.
26. Crowley T, O'Neil JD, Adams H, Thomas AM, Filer A, Buckley CD, et al. Priming in response to pro-inflammatory cytokines is a feature of adult synovial but not dermal fibroblasts. Arthritis Research & Therapy. 2017;19(1):35.
27. Al-Rikabi AHA, Tobin DJ, Riches-Suman K, Thornton MJ. Dermal fibroblasts cultured from donors with type 2 diabetes mellitus retain an epigenetic memory associated with poor wound healing responses. Scientific Reports. 2021;11(1):1474.
28. Wu D, Pan W. GSK3: a multifaceted kinase in Wnt signaling. Trends Biochem Sci. 2010;35(3):161-8.
29. Whyte JL, Smith AA, Helms JA. Wnt signaling and injury repair. Cold Spring Harb Perspect Biol. 2012;4(8):a008078.
30. Simone TM, Longmate WM, Law BK, Higgins PJ. Targeted Inhibition of PAI-1 Activity Impairs Epithelial Migration and Wound Closure Following Cutaneous Injury. Adv Wound Care (New Rochelle). 2015;4(6):321-8.
31. Yazdanpanah L, Shahbazian H, Nazari I, Arti HR, Ahmadi F, Mohammadianinejad SE, et al. Incidence and Risk Factors of Diabetic Foot Ulcer: A Population-Based Diabetic Foot Cohort (ADFC Study)-Two-Year Follow-Up Study. Int J Endocrinol. 2018;2018:7631659.
32. Del Core MA, Ahn J, Lewis RB, Raspovic KM, Lalli TAJ, Wukich DK. The Evaluation and Treatment of Diabetic Foot Ulcers and Diabetic Foot Infections. Foot & Ankle Orthopaedics. 2018;3(3):2473011418788864.
33. Patel BK, Patel KH, Huang RY, Lee CN, Moochhala SM. The Gut-Skin Microbiota Axis and Its Role in Diabetic Wound Healing-A Review Based on Current Literature. Int J Mol Sci. 2022;23(4).
34. Morris JL, Bridson TL, Alim MA, Rush CM, Rudd DM, Govan BL, et al. Development of a diet-induced murine model of diabetes featuring cardinal metabolic and pathophysiological abnormalities of type 2 diabetes. Biology Open. 2016;5(8):1149-62.
35. Hodgson K, Govan B, Ketheesan N, Morris J. Dietary composition of carbohydrates contributes to the development of experimental type 2 diabetes. Endocrine. 2013;43(2):447-51.

36. Parkman JK, Mao X, Dillon K, Gudivada A, Moustaid-Moussa N, Saxton AM, et al. Genotype-dependent Metabolic Responses to Semi-Purified High-Sucrose High-Fat Diets in the TALLYHO/Jng vs. C57BL/6 Mouse during the Development of Obesity and Type 2 Diabetes. Exp Clin Endocrinol Diabetes. 2016;124(10):622-9.
37. Fallah M, Viklund E, Bäckman A, Brodén J, Lundskog B, Johansson M, et al. Plasminogen is a master regulator and a potential drug candidate for the healing of radiation wounds. Cell Death & Disease. 2020;11(3):201.
38. Nogueira G, Solon C, Carraro RS, Engel DF, Ramalho AF, Sidarta-Oliveira D, et al. Interleukin-17 acts in the hypothalamus reducing food intake. Brain Behav Immun. 2020;87:272-85.
39. Araújo EP, De Souza CuT, Ueno M, Cintra DE, Bertolo MB, Carvalheira JB, et al. Infliximab Restores Glucose Homeostasis in an Animal Model of Diet-Induced Obesity and Diabetes. Endocrinology. 2007;148(12):5991-7.

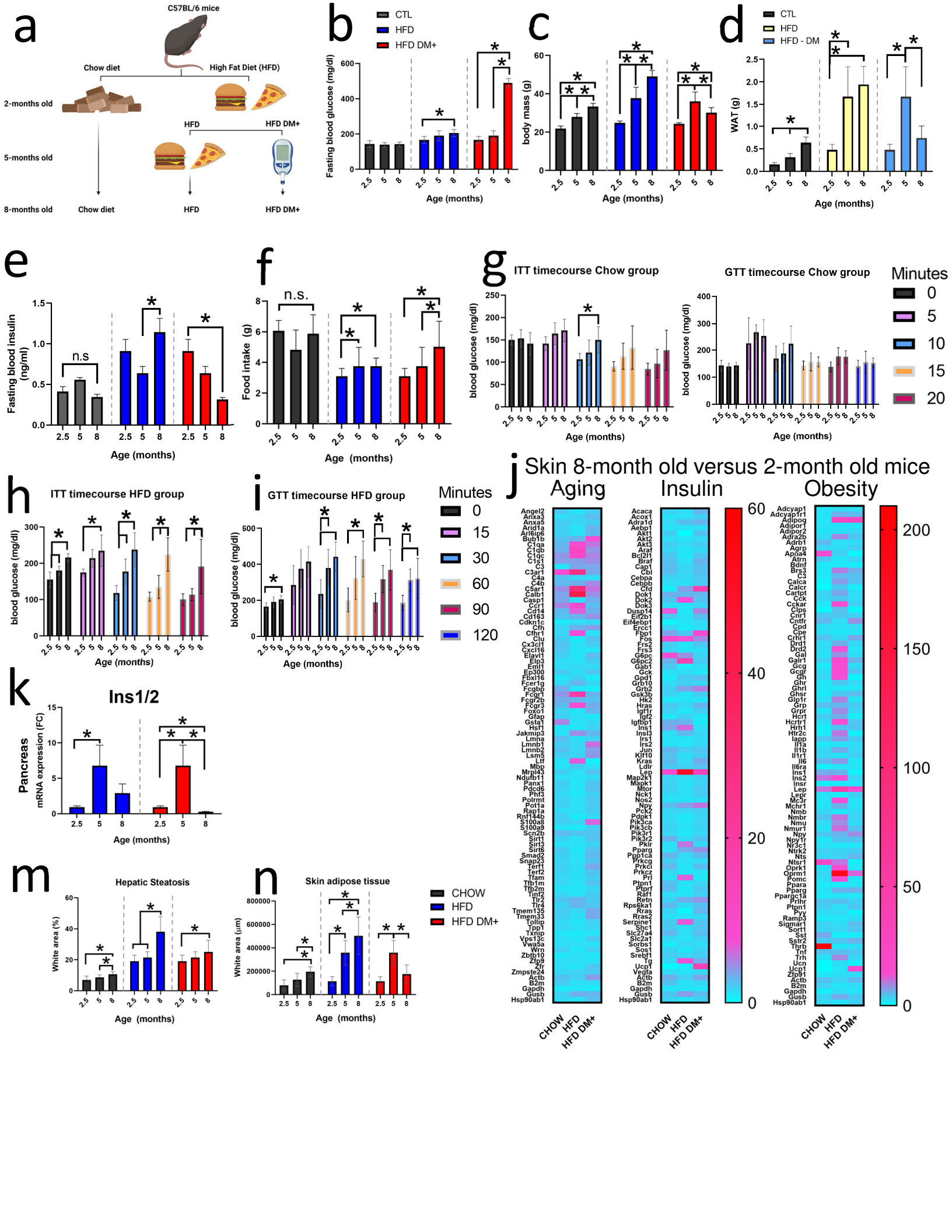
a
C57BL/6 mice
Chow diet
High Fat Diet (HFD)
2-months old
HFD
HFD DM+
5-months old
8-months old
Chow diet
HFD
HFD DM+
b
CTL
HFD
HFD DM+
Fasting blood glucose (mg/dl)
Age (months)
c
body mass (g)
Age (months)
d
CTL
HFD
HFD - DM
WAT (g)
Age (months)
e
Fasting blood insulin (ng/ml)
n.s
Age (months)
f
n.s.
Food intake (g)
Age (months)
g
ITT timecourse Chow group
GTT timecourse Chow group
blood glucose (mg/dl)
Age (months)
Minutes
0
5
10
15
20
h
ITT timecourse HFD group
blood glucose (mg/dl)
Age (months)
i
GTT timecourse HFD group
blood glucose (mg/dl)
Age (months)
Minutes
0
15
30
60
90
120
j
Skin 8-month old versus 2-month old mice
Aging
Insulin
Obesity
CHOW
HFD
HFD DM+
k
Ins1/2
Pancreas
mRNA expression (FC)
Age (months)
m
Hepatic Steatosis
White area (%)
Age (months)
n
Skin adipose tissue
White area (µm)
Age (months)
CHOW
HFD
HFD DM+

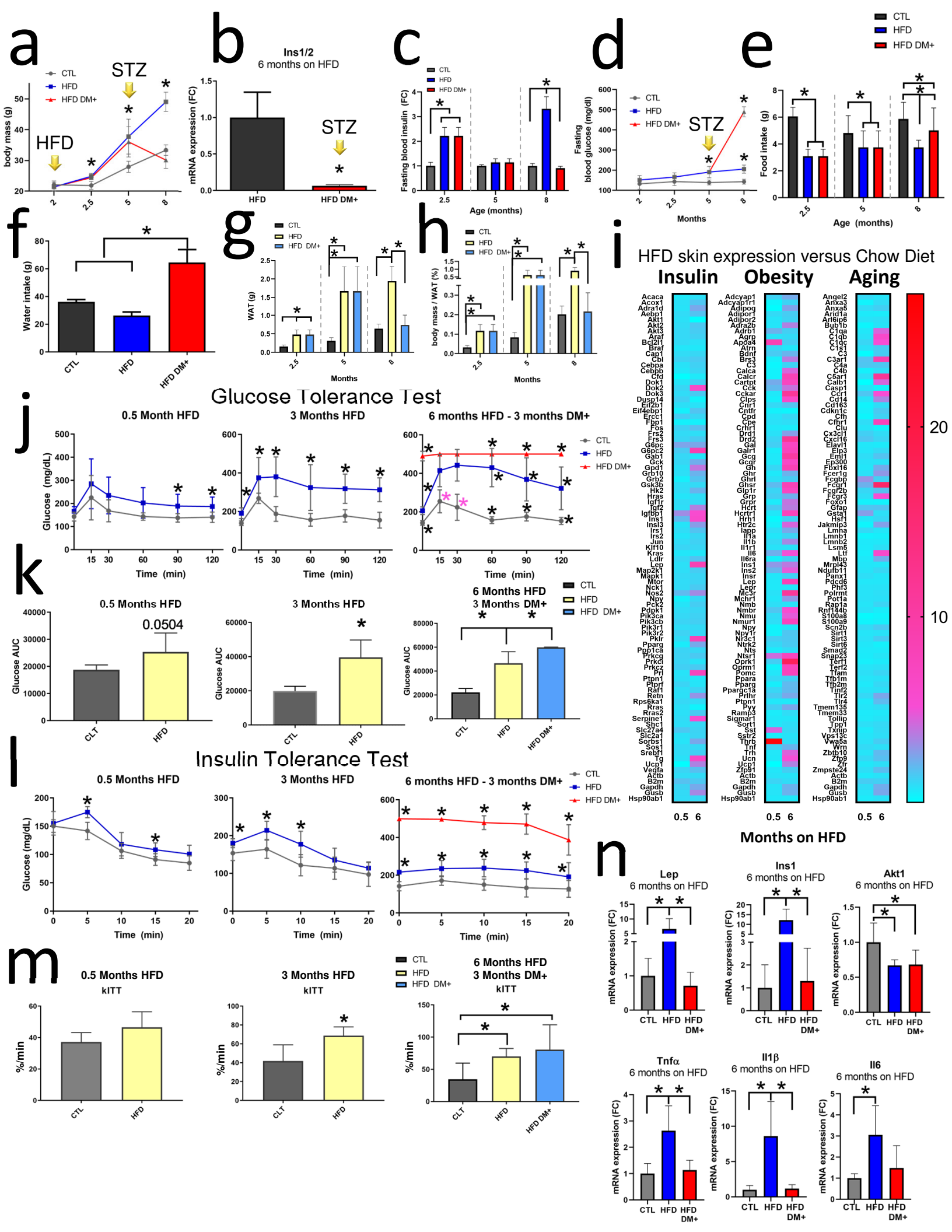
a
CTL
HFD
HFD DM+
STZ
HFD
body mass (g)
b
Ins1/2
6 months on HFD
mRNA expression (FC)
STZ
HFD
HFD DM+
c
CTL
HFD
HFD DM+
Fasting blood insulin (FC)
Age (months)
d
CTL
HFD
HFD DM+
STZ
Fasting blood glucose (mg/dl)
Months
e
CTL
HFD
HFD DM+
Food intake (g)
Age (months)
f
Water intake (g)
CTL
HFD
HFD DM+
g
CTL
HFD
HFD DM+
WAT (g)
Months
h
CTL
HFD
HFD DM+
body mass / WAT (%)
Months
i
HFD skin expression versus Chow Diet
Insulin
Obesity
Aging
Months on HFD
j
Glucose Tolerance Test
0.5 Month HFD
3 Months HFD
6 months HFD - 3 months DM+
Glucose (mg/dL)
Time (min)
CTL
HFD
HFD DM+
k
0.5 Months HFD
0.0504
3 Months HFD
6 Months HFD
3 Months DM+
Glucose AUC
CLT
HFD
CTL
HFD
HFD DM+
l
Insulin Tolerance Test
0.5 Months HFD
3 Months HFD
6 months HFD - 3 months DM+
Glucose (mg/dL)
Time (min)
CTL
HFD
HFD DM+
m
0.5 Months HFD
kITT
3 Months HFD
kITT
6 Months HFD
3 Months DM+
kITT
%/min
CTL
HFD
HFD DM+
n
Lep
6 months on HFD
Ins1
6 months on HFD
Akt1
6 months on HFD
Tnfα
6 months on HFD
Il1β
6 months on HFD
Il6
6 months on HFD
mRNA expression (FC)
CTL
HFD
HFD DM+

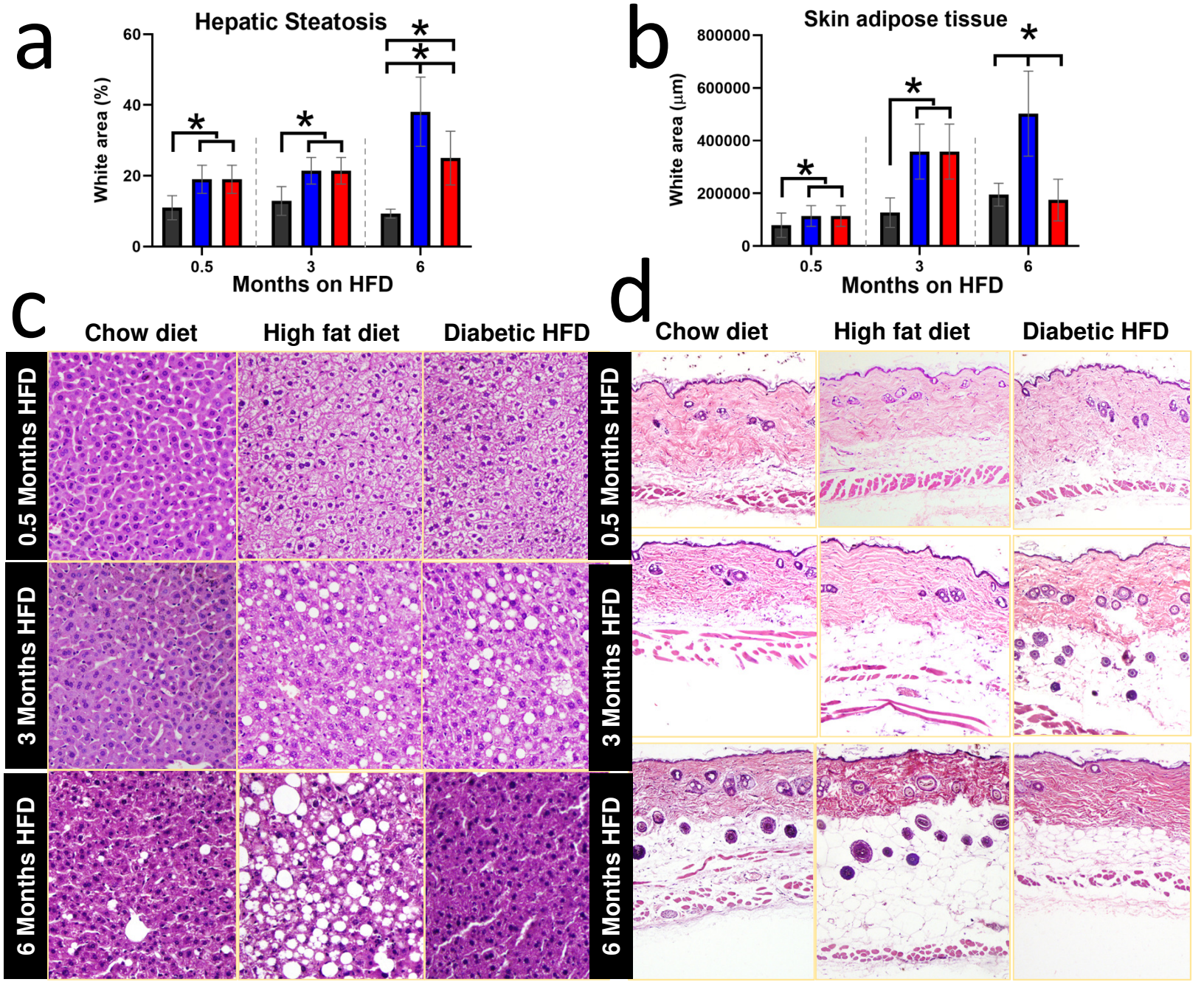
a
Hepatic Steatosis
White area (%)
60
40
20
0
*
*
*
*
0.5
3
6
Months on HFD
b
Skin adipose tissue
White area (μm)
800000
600000
400000
200000
0
*
*
*
0.5
3
6
Months on HFD
c
Chow diet
High fat diet
Diabetic HFD
0.5 Months HFD
3 Months HFD
6 Months HFD
d
Chow diet
High fat diet
Diabetic HFD
0.5 Months HFD
3 Months HFD
6 Months HFD

a
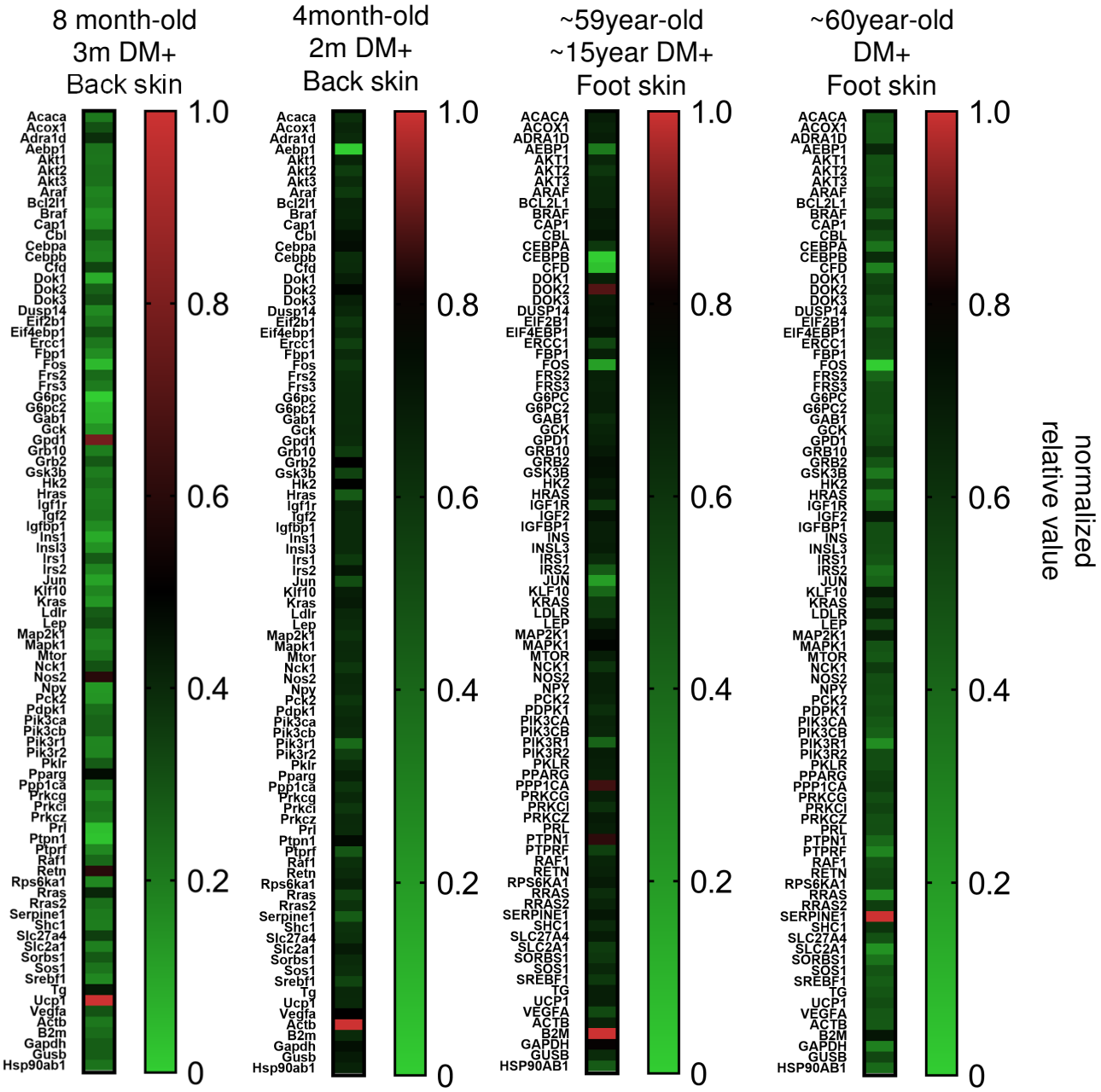
# Diabetic versus Healthy skin (no wounds)